

Intracavity laser spectroscopy using a $\text{Cr}^{2+} : \text{ZnSe}$ laser

V.A. Akimov, V.I. Kozlovskii, Yu.V. Korostelin, A.I. Landman, Yu.P. Podmar'kov, M.P. Frolov

Abstract. A $\text{Cr}^{2+} : \text{ZnSe}$ laser emitting 100- μs pulses tunable in the 2–3- μm region is used for the first time for the highly sensitive detection of absorption spectra by the method of intracavity laser spectroscopy. The intracavity absorption spectra of the atmospheric air were recorded at different instants of lasing in the spectral region from 2.41 to 2.46 μm . An increase in the sensitivity of the laser emission spectrum to intracavity absorption was observed over the entire range of lasing durations studied.

Keywords: intracavity laser spectroscopy, solid-state lasers, $\text{Cr}^{2+} : \text{ZnSe}$ laser.

1. Introduction

At present there is a tendency to extend the spectral range of highly sensitive laser absorption methods (diode spectroscopy, acoustooptic spectroscopy, spectroscopy based on the radiation decay in a laser cavity [1–3]) to the IR spectral region. This is caused by the quest to achieve lower detection thresholds for gases, of which many have relatively intense absorption lines in the IR range. The intracavity laser spectroscopy (ILS) [4] is not an exception in this sense.

The ILS assumes the use of broadband lasers, in which the homogeneous width of the gain band is much greater than the width of the absorption line under study. The most significant advance of the ILS to the IR region was achieved with the help of a $\text{Li} : \text{KCl}$ colour centre laser. The authors of Ref. [5] used this laser to record the intracavity absorption spectrum of the atmosphere in the region of 2.63 μm . Unfortunately, experiments with such lasers involve considerable difficulties due to the instability of colour centres and the necessity to cool strongly the laser crystal.

A substantial progress in the ILS development in the IR region was achieved using a $\text{Co} : \text{MgF}_2$ laser [6, 7], which is tunable in the region between 1.6 and 2.5 μm and can operate at room temperature. However, the room-tempera-

ture operation of the laser requires a high pump power, which severely complicates the generation of long laser pulses needed to achieve the maximum sensitivity of the ILS.

Chalcogenide crystals doped with Cr^{2+} ions are promising active media for broadband IR lasers [8, 9]. In particular, the efficient lasing in the 2–3- μm spectral region was demonstrated in $\text{Cr}^{2+} : \text{ZnS}$ [8, 9], $\text{Cr}^{2+} : \text{ZnSe}$ [9], $\text{Cr}^{2+} : \text{CdSe}$ [10] and $\text{Cr}^{2+} : \text{CdMnTe}$ crystals [11]. These crystals have large homogeneous gain bands and possess good thermo-optical parameters. They also have a convenient absorption band, which can be pumped by semiconductor lasers, operate at room temperature in pulsed and cw regimes, and feature low lasing thresholds and a high efficiency. Due to these properties, these crystals are promising for the development of compact and low cost intracavity IR laser spectrometers.

In this paper, we study for the first time the spectral and kinetic characteristics of a broadband $\text{Cr}^{2+} : \text{ZnSe}$ laser as applied to the ILS problems.

2. Experimental

We performed experiments using the setup built on the basis of the equipment that was employed earlier for recording intracavity absorption spectra with the help of a $\text{Co} : \text{MgF}_2$ laser [6, 7]. The optical scheme of the setup is shown in Fig. 1.

The $\text{Cr}^{2+} : \text{ZnSe}$ laser cavity consisted of mirrors M1 and M2 with the radii of curvature of 200 mm, which were

V.A. Akimov, V.I. Kozlovskii, Yu.V. Korostelin, A.I. Landman, Yu.P. Podmar'kov, M.P. Frolov P.N. Lebedev Physics Institute, Russian Academy of Sciences, Leninsky prosp. 53, 119991 Moscow, Russia; e-mail: frolovmp@x4u.lebedev.ru

Received 1 August 2003

Kvantovaya Elektronika 34 (2) 185–188 (2004)

Translated by M.N. Sapozhnikov

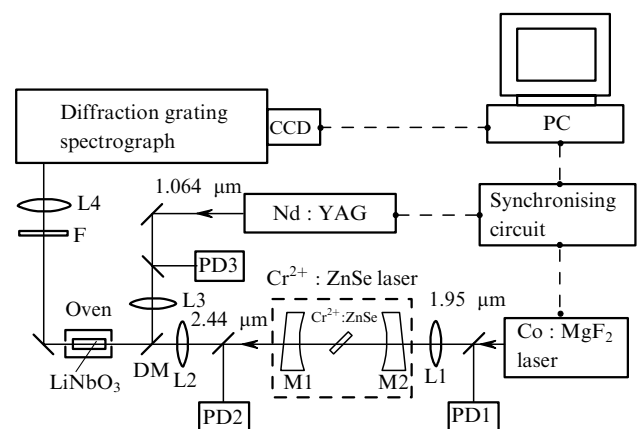


Figure 1. Scheme of the experimental setup.

spaced 365 mm apart. The transmission of the output mirror M1 at a wavelength of 2.44 μm was 2.2 %, the reflectivity of the rear mirror M2 was close to 100 % in the region between 2.3 and 2.8 μm .

The 2.9-mm thick active element of the laser with transverse dimensions of 10×10 mm and thickness of 2.9 mm was made of a $\text{Cr}^{2+}:\text{ZnSe}$ single crystal (the concentration of Cr^{2+} ions was $5 \times 10^{18} \text{ cm}^{-3}$), which was grown from a vapour phase and doped with Cr^{2+} during its growth [12]. The active element was placed in the middle of the cavity at the Brewster angle. The $\text{Cr}^{2+}:\text{ZnSe}$ laser was pumped by a $\text{Co}:\text{MgF}_2$ laser at 1.95 μm . The longitudinal pump scheme was used, in which the beam of the $\text{Co}:\text{MgF}_2$ laser was focused by lens L1 and passed through mirror M2. The pump-spot diameter at the centre of the $\text{Cr}^{2+}:\text{ZnSe}$ crystal was 0.6 mm. The pump radiation energy incident on the crystal was 7 mJ, the output energy of the $\text{Cr}^{2+}:\text{ZnSe}$ laser was 350 μJ , and the maximum of the laser emission spectrum was located at 2.44 μm .

The pump and output pulses of the $\text{Cr}^{2+}:\text{ZnSe}$ laser were detected with PD1 and PD2 photodiodes (InAsSbP/InAs PD36 photodiodes). Figure 2 shows typical pump and output pulses.

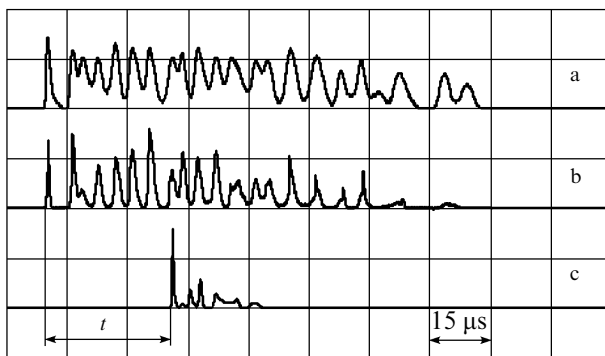


Figure 2. Oscillograms of pump (a) and output pulses from the $\text{Cr}^{2+}:\text{ZnSe}$ laser (b) and the narrowband Nd:YAG laser (c); t is the time measured from the leading edge of the first spike of laser emission.

We could not detect directly the IR emission of the $\text{Cr}^{2+}:\text{ZnSe}$ laser due to the lack of a multichannel IR detector. For this reason, the broadband IR emission from the $\text{Cr}^{2+}:\text{ZnSe}$ laser was converted to visible emission at 740 nm, whose spectrum was recorded using a spectrograph equipped with a CCD linear array coupled with a PC. The nonlinear optical conversion of IR emission to the visible region was performed in a LiNbO_3 crystal by mixing with the 1.064- μm monochromatic radiation from a Nd:YAG laser with the spectral width of 0.02 cm^{-1} . The output energy of the Nd:YAG laser was 5 mJ. To provide the 90° phase matching, the LiNbO_3 crystal was heated up to $\sim 500^\circ\text{C}$ in an oven. The beams from $\text{Cr}^{2+}:\text{ZnSe}$ and Nd:YAG lasers were focused and combined inside the lithium niobate crystal with the help of lenses L2 and L3 and dichroic mirror DM, which transmitted radiation at 2.44 μm and totally reflected light at 1.064 μm . The converted radiation was selected with a glass filter F and focused by the lens L4 on the entrance slit of the diffraction grating spectrograph with a theoretical spectral resolution of 0.04 cm^{-1} .

Because the duration of radiation from the Nd:YAG laser is shorter than that for the $\text{Cr}^{2+}:\text{ZnSe}$ laser, the frequency conversion to the visible region allowed us to record time-resolved spectra. The shape of a pulse from the Nd:YAG laser was detected with a PD3 photodiode (LPD-2A avalanche photodiode). The typical oscillogram is shown in Fig. 2c. The total duration of the pulse from the Nd:YAG laser was approximately 15 μs . However, the first spike of duration $\sim 15 \mu\text{s}$ contained $\sim 50\%$ of the output energy. By varying the delay of the pulse from the Nd:YAG laser with respect to the pump pulse by means of a synchronising circuit, we recorded the emission spectrum of the $\text{Cr}^{2+}:\text{ZnSe}$ laser at any moment t with respect to the leading edge of the laser pulse, thereby observing time-resolved intracavity absorption spectra.

3. Experimental results and discussion

We studied the emission spectra of the broadband $\text{Cr}^{2+}:\text{ZnSe}$ laser, whose resonator was filled with atmospheric air. The spectra were recorded in the range from 2.41 to 2.46 μm for lasing durations from 0 to 100 μs . The spectra obtained for $t = 0$ (the first lasing spike), 10, 20, 40, and 60 μs are presented in Fig. 3a. All the spectra were recorded by accumulating the emission spectra for 100 laser pulses. The spread in the values of t upon averaging was $\pm 3 \mu\text{s}$. The observed absorption is caused by water vapours, whose partial pressure was 5 Torr.

If the laser resonator is completely filled with an absorbing substance (as was the case in our setup), then the effective absorption length L_{eff} in the ILS method is equal to the path propagated by light during the lasing time t_g ($L_{\text{eff}} = ct_g$). The lasing time is measured from the instant of achievement of the threshold inversion. In solid-state lasers, where the upper-level lifetime is usually longer than the lifetime of a photon in the cavity, the first lasing spike appears after the lasing development time t_0 . Therefore, the lasing time is $t_g = t_0 + t$, where t is measured from the leading edge of the first lasing spike (Fig. 2). For this reason the intracavity absorption is observed already in the emission spectrum of the first spike.

Figure 3b shows the model absorption spectra of atmosphere, which were calculated for different absorption lengths using the HITRAN spectroscopic database [13] taking the envelope of the laser emission spectrum into account. We assumed in the calculations that the absorption length is $L = c(\Delta t + t)$, where the value $\Delta t = 4 \mu\text{s}$ was chosen to obtain the best fit between the experimental and calculated spectra for $t = 0$. The delay of the leading edge of the pulse from the $\text{Cr}^{2+}:\text{ZnSe}$ laser with respect to that of the pump pulse from the $\text{Co}:\text{MgF}_2$ laser was approximately 1 μs , so that the lasing development time t_0 could not exceed this value. It seems that the value $\Delta t = 4 \mu\text{s}$ is determined not only by the lasing development time t_0 but also by the above-mentioned spread in the delay time t during the averaging of the spectra, as well as by a long total duration (15 μs) of the Nd:YAG laser pulse.

A good qualitative agreement between the calculated and experimental absorption spectra shows that the sensitivity of the emission spectrum of the $\text{Cr}^{2+}:\text{ZnSe}$ laser with respect to intracavity absorption increases in the range of lasing durations from 0 to 100 μs . However, we cannot study quantitatively the linearity of this increase under our experimental conditions for two reasons. First, the observed

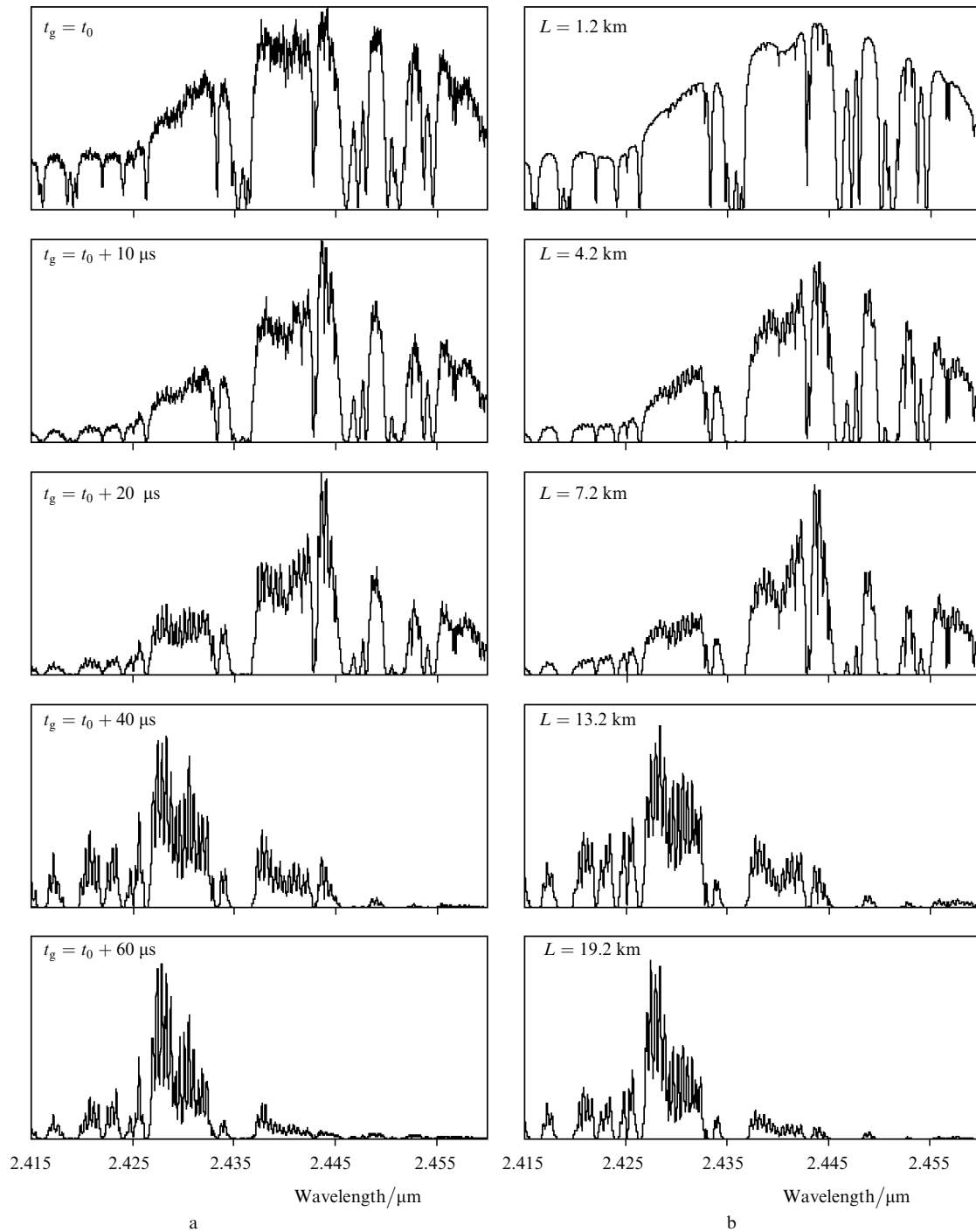


Figure 3. Intracavity absorption spectra of the atmospheric air recorded at different instants of lasing in the $\text{Cr}^{2+} : \text{ZnSe}$ laser (a) and the absorption spectra of the atmospheric air calculated for the partial pressure of water vapours equal to 5 Torr for different lengths of an absorbing layer taking into account the envelope of the experimental emission spectrum of the $\text{Cr}^{2+} : \text{ZnSe}$ laser (b).

absorption lines are strongly saturated. Therefore, we plan to measure in future the dynamics of intracavity absorption at lower pressures of water vapours, which requires the use of a hermetically sealed cavity. Second, the laser emission spectrum is strongly modulated, which is caused, in our opinion, by interference effects appearing during the propagation of laser radiation through an active element representing a Fabry–Perot etalon (the modulation period of the spectrum equal to 0.76 cm^{-1} coincides with the free spectral range of the etalon formed by the end surfaces of the

$\text{Cr}^{2+} : \text{ZnSe}$ crystal). Figure 4 shows a part of the laser emission spectrum extended along the abscissa, which distinctly demonstrated this modulation. The increase in the modulation amplitude with time also confirms qualitatively the increase in the sensitivity with the lasing duration. However, to study weaker absorption spectra, this modulation should be eliminated. This will probably require the use of a thicker active element or a wedge active element for eliminating the interference of a laser beam with secondary beams reflected from the faces of the active element.

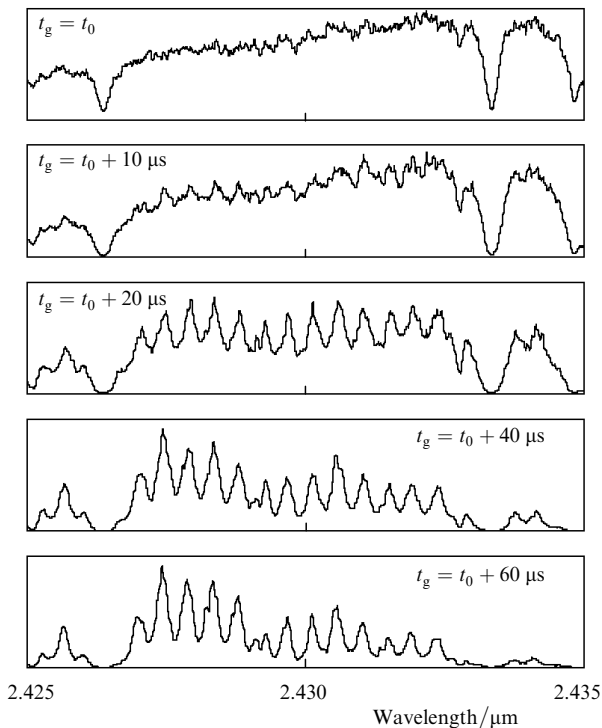


Figure 4. Modulation of the emission spectrum of the $\text{Cr}^{2+} : \text{ZnSe}$ laser due to interference upon reflection of light from the active element surface at different instants of lasing.

4. Conclusions

We have shown that a $\text{Cr}^{2+} : \text{ZnSe}$ laser can be used for the IR intracavity laser spectroscopy. The increase in the sensitivity of the laser emission spectrum to intracavity absorption was observed with increasing lasing duration at least up to 100 μs , which is equivalent to the effective absorbing length equal to 30 km. Thus, we have shown that the $\text{Cr}^{2+} : \text{ZnSe}$ laser can be used for the development of a compact and low cost IR ILS spectrometer.

Acknowledgements. This work was partially supported by the American Civil Research and Development Foundation (a CRDF BRHE REC-011 Grant) and the 'New Materials and Structures' Program of the Fundamental Research, Russian Academy of Sciences.

References

1. Werle P., Popov A. *Appl. Opt.*, **38**, 1494 (1999).
- [doi>](#) 2. Sigrist M.W., Bohren M.W., Calasso I.G., Nägele M., Romann M., Seiter M. *Proc. SPIE Int. Soc. Opt. Eng.*, **4063**, 17 (2000).
- [doi>](#) 3. Berden G., Peeters R., Meijer G. *Int. Rev. Phys. Chem.*, **19**, 565 (2000).
4. Pakhomycheva L.A., Sviridenkov E.A., Suchkov A.F., Titova L.V., Churilov S.S. *Pis'ma Zh. Eksp. Teor. Fiz.*, **12**, 60 (1970).
5. Baev V.M., Dubov V.P., Kireev A.N., Sviridenkov E.A., Toptygin D.D., Yushchuk O.I. *Kvantovaya Elektron.*, **13**, 1708 (1986) [*Sov. J. Quantum Electron.*, **17**, 1121 (1986)].
- [doi>](#) 6. Frolov M.P., Podmar'kov Yu.P. *Opt. Commun.*, **155**, 313 (1998).
- [doi>](#) 7. Podmar'kov Yu.P., Raspopov N.A., Savchenko A.N., Frolov M.P. *Kvantovaya Elektron.*, **28**, 186 (1999) [*Quantum Electron.*, **29**, 742 (1999)].
- [doi>](#) 8. DeLoach L.D., Page R.H., Wilke G.D., Payne S.A., Krupke W.F. *IEEE J. Quantum Electron.*, **32**, 885 (1996).
- [doi>](#) 9. Page R.H., Schaffers K.L., DeLoach L.D., Wilke G.D., Patel F.D., Tassano J.B., Payne S.A., Krupke W.F., Chen K.-T., Burger A. *IEEE J. Quantum Electron.*, **33**, 609 (1997).
10. McKay J., Schepler K., Catella G.C. *Opt. Lett.*, **24**, 1575 (1999).
11. Hommerich U., Wu X., Davis V.R., Trivedi S.B., Graszka K., Chen R.J., Kutcher S. *Opt. Lett.*, **22**, 1180 (1997).
- [doi>](#) 12. Kozlovskii V.I., Korostelin Yu.V., Landman A.I., Podmar'kov Yu.P., Frolov M.P. *Kvantovaya Elektron.*, **33**, 408 (2003) [*Quantum Electron.*, **33**, 408 (2003)].
- [doi>](#) 13. Rothman L.S., Rinsland C.P., Goldman A., Massie S.T., Edwards D.P., Flaud J.-M., Perrin A., Camy-Peyrot C., Dana V., Mandin J.-Y., Schroeder J., McCann A., Gamache R.R., Wattson R.B., Yoshino K., Chance K.V., Jucks K.W., Brown L.R., Nemtchinov V., Varanasi P. The HITRAN molecular spectroscopic database and HAWKS (HITRAN Atmospheric Workstation) (1996 Edition); *J. Quantum Spectrosc. Radiat. Transfer*, **60**, 665 (1998).